Analytica Chimica Acta 1198 (2022) 339557

Contents lists available at ScienceDirect

Analytica Chimica Acta

journal homepage: www.elsevier.com/locate/aca

Paper-based aptasensor for colorimetric detection of osteopontin

Ana Claudia Pereira [a, b, c], Felismina T.C. Moreira [c, *], Ligia R. Rodrigues [a, e], M. Goreti F. Sales [a, c, d]

[a] CEB - Centre of Biological Engineering, University of Minho, Braga, Portugal
[b] MIT-Portugal Program, Lisbon, Portugal
[c] BioMark@UC, Faculty of Sciences and Technology, University of Coimbra, Coimbra, Portugal
[d] BioMark@ISEP, School of Engineering, Polytechnic of Porto, Porto, Portugal
[e] LABBELS –Associate Laboratory, Braga, Guimarães, Portugal

HIGHLIGHTS

- Development of a cellulose-based colorimetric test strip for the detection of a cancer biomarker.
- Aptamer as a biological recognition layer for an OPN detection.
- Bradford as a detection reagent.
- Visual quantitative detection of a cancer biomarker.

GRAPHICAL ABSTRACT

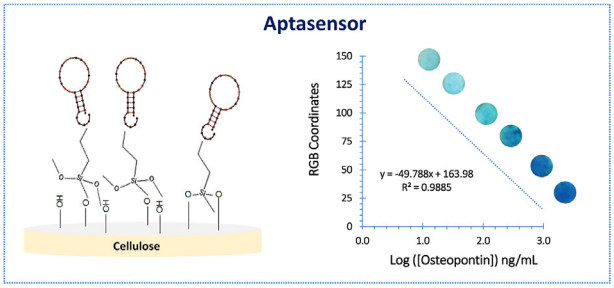

ARTICLE INFO

Article history:
Received 5 October 2021
Received in revised form
5 January 2022
Accepted 25 January 2022
Available online 29 January 2022

Keywords:
Paper-based aptasensor
Colorimetric
Osteopontin
Bradford reagent
Color coordinates

ABSTRACT

This work presents a novel cellulose-based aptasensor for the colorimetric detection of a cancer biomarker, osteopontin (OPN), in point-of-care (PoC) analysis.

For this purpose, the cellulose paper was chemically modified with (mercaptopropyl)methyldimetoxisilane to attach the thiolated aptamer, which acts as a biological detection layer. The surface modification was checked by Fourier transform infrared spectroscopy and thermogravimetric analysis. Colorimetric detection was performed using a conventional staining solution, Bradford reagent. The color analysis was performed by evaluating the RGB coordinates provided by the *ImageJ* program from the photographs taken with a smartphone.

Overall, the biosensor shows good sensitivity with a wide linear range ($R > 0.998$) of 5–1000 ng/mL and a detection limit lower than 5 ng/mL in buffer and commercial human serum solution, after 30 min of incubation. In addition, this aptasensor shows good selectivity to some interfering species such as bovine serum albumin and recombinant OPN. Analytical data obtained from spiked serum samples confirm the accuracy of the method.

Importantly, it is a broad-spectrum method that tends to meet the criteria of REASSURED (real-time connectivity, ease of sampling, affordability, specificity, ease of use, speed and robustness, device freedom, and deliverability) for global testing.

© 2022 Elsevier B.V. All rights reserved.

* Corresponding author. School of Engineering of the Polytechnic School of Porto, R. Dr. António Bernardino de Almeida, 431, 4249-015, Porto, Portugal.
E-mail address: ftm@isep.ipp.pt (F.T.C. Moreira).

https://doi.org/10.1016/j.aca.2022.339557
0003-2670/© 2022 Elsevier B.V. All rights reserved.

1. Introduction

Paper-based devices, as far as cost goes, remain one of the best options for PoC use [1]. It entails advantages like portability, sensitivity, specificity, user-friendly and equipment independency [2], without compromising affordability. Moreover, because of cellulose's physical and chemical flexibility, these types of devices allow limitless modifications in their architecture, making them very attractive for clinical diagnostics [1]. Within this type of sensors, the ones employing aptamers as biorecognition elements are particularly attractive, since it extends further the affordability of the device [3]. In fact, because aptamers have higher stability than antibodies and are easily modifiable, they represent a much more attractive option as recognition elements [4].

Of all the detection techniques used in biosensors, the colorimetric response is an attractive approach because of its ease of reading and analysis. It allows both a qualitative response, which can be answered "yes" or "no", and a quantitative response, where there is a correlation between the concentration of the analyte and the colorimetric signal. Therefore, there is an increasing interest in the use of smartphones as quantification systems, mainly because of their accessibility, portability and ease of use [5–7]. Smartphones are a widely used class of device, so their use as a diagnostic tool at minimal cost is a great advantage [8].

Therefore, an increasing number of studies are reported in which paper is the substrate, aptamers are the type of biorecognition element and smartphones are the analytical system of biosensors in various research areas such as environmental [9,10], microbiology [11] and health [12–15].

There has been an increasing number of paper-based biosensors for cancer detection that attempt to meet PoC criteria [16]. They use a variety of bio-detection elements and a wide range of transducers, all aiming to expand access to diagnosis worldwide [16,17]. However, when looking only at papers combining paper-based support and aptamers for cancer biomarker screening, the number of papers decreases significantly.

Interestingly, almost all strategies shown in Table S1 present an electrochemical response and use somewhat sophisticated electrode assemblies, like gold nanoparticles [18–20], graphene [18,20–22], specific 3D structures [21,23,24] or wax printing [25], which question the general affordability of PoC devices. Other approaches use surface-enhanced Raman scattering, in which gold nanourchins functionalized with an aptamer for cytochrome *c* and with cyanine-5-labelled complementary DNA are attached to a paper surface [26], allowing high sensitivity. However, this approach is not suitable for PoC analysis. The laser-induced fluorescence sensor for the detection of miRNA-21 and miRNA-31, which is based on duplex-specific nuclease amplification, was able to detect the two miRNAs in cancer cells in the femto range [27]. However, like the previous method, it is not suitable for PoC applications. The colorimetric approach developed by Mukama et al. represents an interesting lateral flow method that achieves limits of detection (LoD) for OPN compatible with clinical requirements [28]. This approach represents a PoC possibility, although the use of antibodies compromises stability and storability.

Thus, the aim of this work is therefore to develop an affordable biosensor that meets PoC requirements, is easily scalable and suitable for clinical practice. For this purpose, cellulose was used as substrate and an aptamer as recognition element. OPN was chosen as the target protein for our platform because it has shown promising results as a breast cancer biomarker and has a range of clinical values [29] with direct correlation with the development of the disease, metastasis and poor prognosis [29–32], even in Triple Negative Breast Cancer (TNBC) [33]. Herein, for the detection system, a color development with the Bio-Rad reagent was used and captured next with a smartphone's camera for further protein quantification.

2. Experimental section

2.1. Reagents and equipment

All reagents used are of analytical grade and all aqueous solutions were prepared with Mili-Q water. The cellulose used was Fanoia S300 from Anoia. Ethanol absolute (C_2H_5OH) was purchased from Honeywell, acetone (CH_3COCH_3) from LabChem and acetic acid glacial (CH_3COOH) from Carlo Erba. 3-(mercaptopropyl) methyldimetoxisilane ($CH_3Si(OCH_3)_2CH_2CH_2CH_2SH$) (MTS), as well as Bovine serum albumin (BSA) and Dithiothreitol (DTT) were acquired from Sigma Aldrich and phosphate buffered saline (PBS) tablets were obtained from Amresco, dissolved in Mili-Q water according to the brand recommendations and then, pH was changed to 7.2 and pH 5.0 to carry on with the required experiments. Recombinant bovine OPN (rbOPN) was purchased from R&D Systems and recombinant human OPN (rhOPN) was acquired from Bio-Techne. The OPN aptamer (5′-Thiol-AAAAAAAAAA TGT GTG CGG CAC TCC AGT CTG TTA CGC CGC-3′) was synthetized by Alfagene. Commercial human serum was purchased from Cormay® and used undiluted for the selectivity assays. Protein assay dye concentrate was obtained from Bio-Rad and was used without dilution.

A Fourier Transform Infrared (FTIR) spectrometer from Thermo Scientific (Nicolet iS10), with an ATR (attenuated total reflectance) accessory with a diamond crystal, and thermogravimetry (TG) in a Hitachi TG/DTA 7200 Exstar were used to follow up the chemical modifications in the S300 cellulose.

2.2. Aptasensor construction

2.2.1. Chemical modification of the cellulose

Fanoia S300 paper was cut into 6 mm diameter circles and suspended in absolute ethanol for 2 h to remove impurities. Then the cellulose surface, which normally contains hydroxyl functions, was modified to contain thiol groups. This was done by incubating the cellulose substrate with MTS, which was prepared in different solvents (i) absolute ethanol, (ii) acetone, (iii) glacial acetic acid and (iv) absolute ethanol/water (80:20). Different concentrations of MTS were tested in each of these solvents: 1.0, 2.5, 5.0 and 10.0%. The cellulose strips were incubated in each solvent for 2, 3 and 4 h respectively at room temperature with gentle agitation. The paper circles were then treated at 50, 60, 70, 90, 110 or 130 °C for 2, 3 and 4 h, followed by washing with absolute ethanol for 10 min and air drying overnight. The functionalization of the cellulose was monitored by FTIR with spectra ranging from 400 to 4000 cm^{-1}, a resolution of 2 cm-1 and an accumulation of 250 scans after background acquisition. Thermogravimetric analysis (TG) was carried out at a temperature range of 30 °C to 500 °C at a rate of 5 °C/min in an aluminium tub. The best conditions were then selected by univariate optimization.

2.2.2. Aptamer immobilization

The next step consisted in assembling the biorecognition layer on the previously functionalized cellulose paper. A thiol modified aptamer that could bind OPN via the thiol groups [29], was used for this purpose. Prior to immobilization, the aptamer was first diluted in PBS, pH 7.2, at 500 nM and heated at 95 °C for 5 min. Afterwards, DTT was added to the aptamer solution to a final concentration of 1.0 μM, to keep free the disulfide bonds in the aptamer structure. Next, 20 μL aliquots were dropped on top of the paper and left to incubate at room temperature for 2, 3, 4 and 24 h, under humectant

conditions. Finally, the unbounded aptamers were rinsed with deionized water and the papers left to air dry before FTIR analysis.

2.3. Dye for color development

For the detection of the rhOPN protein, the Bio-Rad Protein Assay Dye was used at various dilutions (1:1, 1:2; 1:3; 1:4; 1:5; in water) and poured onto papers. The papers used here represented the different stages of functionalization (after washing with ethanol, after silanization curing and after immobilization of the aptamer) to determine the best dilution. The digital images of the color development were taken with a smartphone camera under controlled light and the corresponding RGB color coordinates (red, green, blue) were analyzed with *ImageJ* software.

2.4. Osteopontin detection in buffer and human serum

After selecting the best concentration of Bio-Rad reagent, 20 μL of a fixed concentration of 100 ng/mL rhOPN protein was added to each test strip to ensure a suitable LoD. After 15 min of incubation, 30 μL of the Bio-Rad reagent was dropped onto the strips and allowed to dry completely at room temperature. Standard solutions of rhOPN protein ranging from 5 to 1000 ng/mL were then prepared in PBS pH 7.4 and in Cormay® human serum for OPN detection. Then, 20 μL of each standard solution was dropped onto the aptamer-functionalized test strips and incubated at room temperature for 30 min. Subsequently, each test strip was rinsed with PBS and color development was observed over a period of 30 min. The pictures from the standards test-strips were taken all together and at the same time, in a black chamber. A circular and constant colored area of the collected images underwent ImageJ evaluation. The values of the characteristic coordinates provided by ImageJ were evaluated and the red coordinate was plotted against OPN concentration to obtain a linear trend. All experiments were performed in triplicate. The LoD was considered below the linear range observed, as all standards were included in the linear range.

2.5. Selectivity study

For the selectivity studies, BSA and rbOPN were tested in both PBS and Cormay® serum under the same conditions as described in Section 2.3. Each of the interfering proteins was incubated in the aptasensor as a single experiment to evaluate color development. For data analysis, the color coordinates were evaluated using the same software and compared to those of the target protein and control.

3. Results and discussion

3.1. Chemical modification of the cellulose

Different solvents were tested to determine the solubility of MTS. The mixture of absolute ethanol and water showed poor results, while acetic acid, acetone and absolute ethanol proved to be good solvents for the silane compound and were therefore chosen to prepare the silane solution (Fig. S1). The best solvent was chosen to determine different temperatures between 50 and 130 °C for the curing step (Fig. S2). After determining the best curing temperature, different concentrations ranging from 1.0 to 10.0% of MTS were prepared to determine the optimal MTS concentration for this step of chemical modification of the cellulose (Fig. S3).

Confirmation of the silane-based modification on the cellulose substrate was done by FTIR analysis. For comparison purposes, the FTIR spectra of the reagent MTS (without silanization) were also evaluated at each step and added to the spectra. Overall, the cellulose substrates incubated for 2 h with MTS at 10% in absolute ethanol with a curing step at 110 °C for 3 h showed similar parts to the FTIR spectra of MTS and distinct features compared to the washed untreated paper (**grey-shaded areas in** Fig. S1, Fig. S2 and Fig. S3).

The MTS spectra show in detail the interesting peaks related to the vibrations of the silicon bonds. However, due to the low sensitivity of the infrared spectrum for thiol groups, it was not possible to identify them in the solution MTS or in the cellulose samples by FTIR. For this reason, the success of chemical modification of cellulose with MTS was first estimated by signaling the rising peaks of silicon bonds at 1260 cm^{-1} (Si–C) [34] and between 1100 cm^{-1} and 650 cm^{-1} (Si–OH, Si–C and Si–O–Si) [34]. As shown in Fig. S1 – S3, increasing concentrations of MTS provided increased intensity signal at 1260 cm^{-1}, at 1100 cm^{-1} and between 840 and 720 cm^{-1} (light grey zones in Fig. S1 – S3), suggesting the presence of the silane groups and, therefore, the functionalization of the surface of the S300 cellulose. Higher concentration of MTS enhanced the signal in the above wavebands, with the spectra losing the profile of the washed paper and showing similarities to the spectra of the MTS solution. These results are consistent with previous studies investigating the interactions between cellulose fibers and silanes, where the chemistry of these interactions can be compared to those observed between glass fibers and silanes under high temperature conditions [35].

Thermogravimetry (TG) has also been used as a complementary analytical tool to track chemical changes. Derived thermogravimetric (DTG) and thermogravimetric (TG) profiles are shown in Fig. 1 and show the mass loss and degradation profile of washed (control) and silanized cellulose paper.

The mass loss from 30 to about 280 °C was about 11% for the control sample, while it was about 6% for the silanized sample. This is mainly due to evaporation of water and ethanol. For the washed paper (control), the second and most significant weight loss occurred between 300 and 385 °C, which corresponded to 76% of the original mass, with a decomposition peak occurring at 353 °C, which can be attributed to the decomposition of cellulosic and non-cellulosic materials. The maximum decomposition of the silanized paper occurred at 351 °C, with about 81% of the original mass lost. The difference observed in the first weight loss for the two samples agrees well with other reports in the literature and confirms that a higher percentage of the material was thermally stable, which can be attributed to the presence of the silane film [34]. However, when considering the overall mass loss, one would expect a higher residual mass for the silanized sample due to the remaining silane film. One possible explanation is that, contrary to what is reported in the literature [36], the silane compound was dissolved in absolute ethanol instead of aqueous solution, which changes the stability of the silane film on the cellulose surface. Nevertheless, both TG and DTG show differences between the two samples, providing a first indication of chemical modification of the cellulose by the silane.

3.2. Aptasensor assembly

After cellulose modification by silanization, an OPN aptamer was covalently immobilized by a disulfide bond between the thiol groups of the silane and the thiol end of the aptamer. To ensure binding of the aptamer to the target molecule, we inserted a 10-adenine spacer at the 5′-end to facilitate exposure of the binding domain and reduce steric hindrance upon OPN binding.

Following the procedure described in the Methods section, we successfully modified the silanized cellulose with the aptamer. The resulting papers were analyzed for complete functionalization by FTIR (Fig. 2).

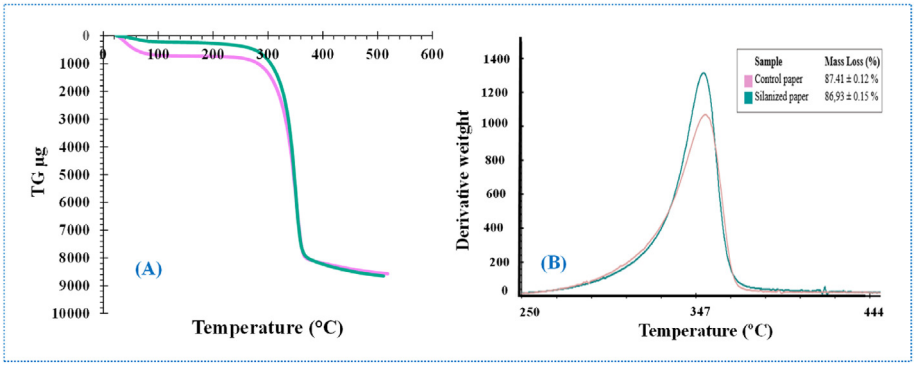

Fig. 1. Thermogram (A) and derivative thermogram (B) of untreated cellulose (control material; pink lines) and chemically modified S300 cellulose with 3-(mercaptopropyl) methyldimetoxisilane (MTS) (green lines). (For interpretation of the references to color in this figure legend, the reader is referred to the Web version of this article.)

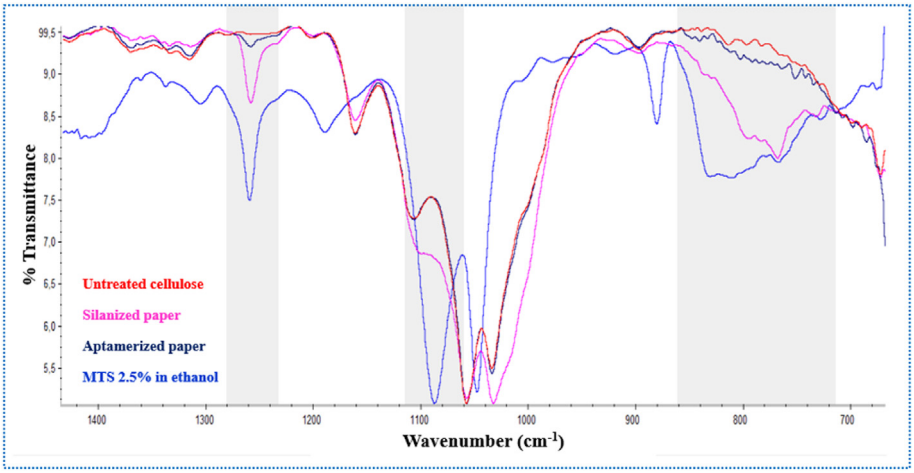

Fig. 2. Fourier Transform Infrared Spectroscopy (FTIR) spectra for the different steps of the biosensor functionalization. The red line represents untreated cellulose; the pink line represents the silanized cellulose with 3-(mercaptopropyl)methyldimetoxisilane (MTS) at 10%; the dark blue line represents the aptamer-silane-functionalized cellulose; and the blue line represents MTS at 2.5% in absolute ethanol in solution. (For interpretation of the references to color in this figure legend, the reader is referred to the Web version of this article.)

When comparing the spectra between the silanized paper and the aptamerized paper, there can be observed a decrease in the peak's intensity after incubation with the aptamer in the same regions analyzed previously in the silanization step. For 1260 cm^{-1}, 1100 cm^{-1} and between 840 and 720 cm^{-1} **(light grey zones in** Fig. 2**),** the peaks represented by silicon bonds decreased their intensity, suggesting a coverage by another compound and, therefore, aptamer immobilization on the cellulose surface.

3.3. Assessment of the color development

A dye suitable for protein quantification, Bio-Rad Protein Assay Dye, was used for color development. The acidic dye, Coomassie® Brilliant Blue G-250, exhibits an absorption maximum at 465 nm. However, in the presence of mainly basic and aromatic amino acid residues, the absorption shifts to 595 nm, resulting in a colorimetric change from red to blue. To this end, different dilutions of the dye were first tested to determine the best concentration to achieve maximum sensitivity. Then, 30 µL of each dilution was dropped onto paper strips representing the different functionalization steps. Finally, the papers were incubated for 15 min, and the excess dye was removed with absorbent paper. Although the dye manufacturer recommends a working dilution of 1:4, the best results were obtained with the concentrated dye, and the resulting color development was captured with the digital smartphone camera under controlled light.

The results showed clear color differences between the papers after washing, after chemical modification and after aptamer incubation (Fig. 3) and confirmed the FTIR data.

According to the supplier, the Bio-Rad dye is a concentrated red dye based on the Bradford method, reacts with primary amines and is sensitive to pH variations. This explains the red color of the washed paper, as primary amines are not present in this sample. Despite the absence of amines, the silanized paper exhibits an acidic character due to the chemical modification, as the pH of the solution was MTS 5.0. The aptamer immobilized on the silanized paper contains primary amines from the nucleotides adenine, guanine and cytosine, which explains the blue color. These results confirm the FTIR data and demonstrate the success of the chemical and functional modifications.

3.4. Analytical performance of the biosensor

3.4.1. Calibration curve in buffer

For target detection, standard solutions of rhOPN were prepared at concentrations ranging from 5 to 1000 ng/mL. Subsequently, 20 µL of each standard solution was incubated in dried optimized aptamer-functionalized papers for 30 min and then washed with

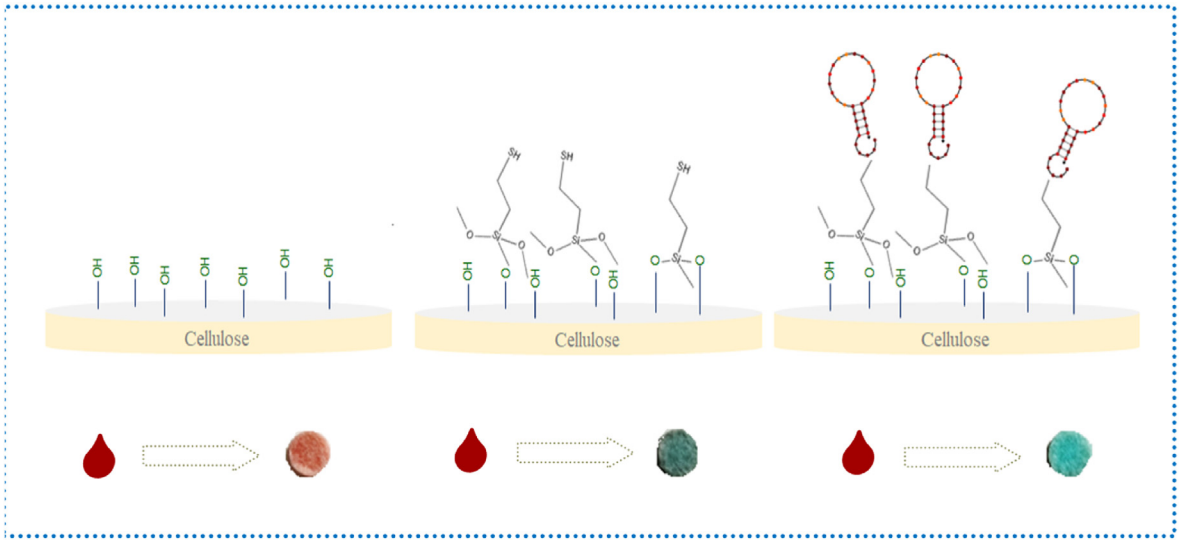

Fig. 3. Representation for the different steps of the biosensor functionalization and respective cellulose color after incubation with the concentrated Bio-Rad dye (red drop). Image on the left represents the untreated cellulose; middle image represents silanized cellulose with 3-(mercaptopropyl)methyldimetoxisilane (MTS) at 10%; and the image on the right represents the aptamer-functionalized cellulose. (For interpretation of the references to color in this figure legend, the reader is referred to the Web version of this article.)

PBS pH 7.4 to remove unbound protein. The PBS excess was removed with absorbent paper, and the color was monitored and recorded with a smartphone camera under controlled light.

The analysis consisted of examining the distribution of the various parameters of the RGB system to establish a correlation between one or more of these parameters and OPN concentration. The first tests performed with the Aptasensor with OPN showed a color change between the control solution (without OPN) and the standard solution (with OPN). However, the color difference between the standard solutions didn't correlate with the increase in OPN concentration. Therefore, an optimization of the sensitivity was necessary. To this end, a fixed concentration of rhOPN was added to the papers containing the immobilized aptamer, followed by addition of the dye and drying at room temperature. This modification of the original setup formed the final aptasensor setup. The presence of a fixed concentration of the target in the sensor allowed it to respond to the addition of small amounts of the target, increasing sensitivity to rhOPN. Since the disclosure medium (dye) was already present in this setup, the number of assay steps could be reduced to only two, namely sample incubation and a wash step. Image-J analysis revealed a correlation between the colorimetric response and the concentration of the target (Fig. 4).

Of all the parameters provided by the ImageJ software, the red coordinate showed the best linear correlation with increasing OPN concentration. Considering the different coordinates and the mathematical system used, the red and green coordinates showed progressive signal decrease, with the red coordinate showing the strongest signal decrease in a wide range of target concentrations. Therefore, this parameter (red coordinate) was selected for analysis. The biosensor showed linearity as a function of concentration between 5 and 1000 ng/mL with a squared correlation coefficient of 0.988.

3.4.2. *Selectivity assessment*

After optimization of the aptasensor, BSA and rbOPN at a concentration of 1000 ng/mL were used as interfering substances, under the same conditions described for rhOPN. Afterwards, the resulting color was captured with a smartphone and the images analyzed by ImageJ software (Fig. 5).

The results showed an 84% signal decrease for the rhOPN at 1000 ng/mL compared to the red coordinate signal of the control, while both BSA and rbOPN showed low affinity to the surface of the

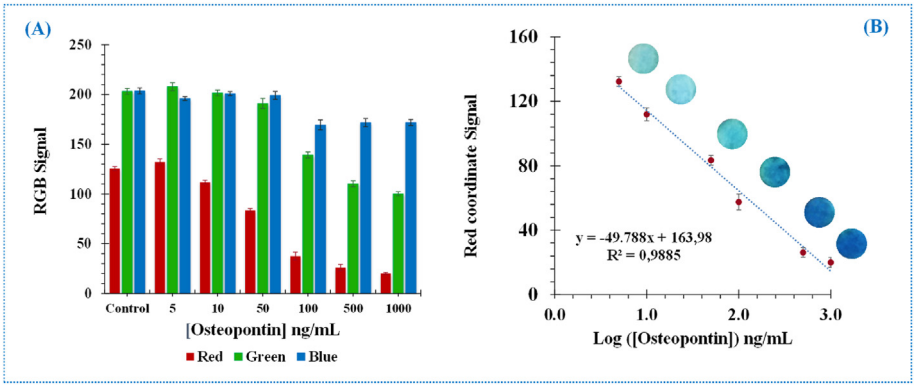

Fig. 4. Calibration curve for Osteopontin (OPN) in phosphate buffered saline (PBS). A: variation of the RGB (Red, Green, Blue) coordinates with the variation of OPN concentration; B: Calibration curve and linear equation for the red coordinates as a logarithm function of OPN's concentration from 5 to 1000 ng/mL. (For interpretation of the references to color in this figure legend, the reader is referred to the Web version of this article.)

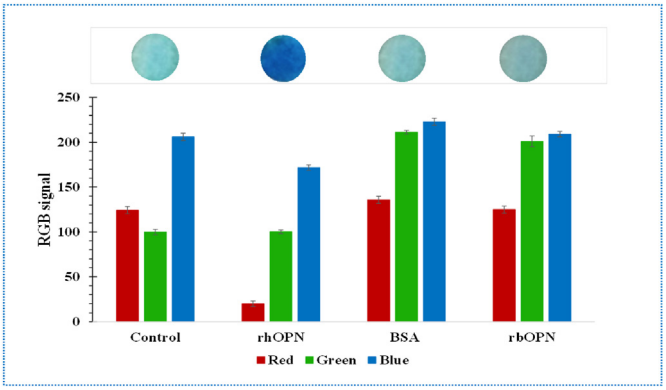

Fig. 5. RGB (Red, Green, Blue) coordinates for phosphate buffered saline (PBS) (control), recombinant human Osteopontin (rhOPN), Bovine Serum Albumin (BSA) and recombinant bovine Osteopontin (rbOPN), at 1000 ng/mL. The aptasensor was incubated with each protein in single-assays and the colors captured for ImageJ analysis. (For interpretation of the references to color in this figure legend, the reader is referred to the Web version of this article.)

biosensor at the same concentration, as the red coordinate value was similar to that of the control (Fig. 5). This is a good result since one of the main problems with using cellulose as a support matrix is its absorption capacity, which often leads to false positive results. In this case, the results seem to support the argument that the OPN signal is correlated with the interaction between the target and its recognition element.

3.4.3. Calibration curve in serum samples

Standard solutions of rhOPN in Cormay® human serum were then prepared to investigate how a complex matrix would affect target recognition and color development. For this purpose, rhOPN solutions were prepared at concentrations ranging from 5 to 1000 ng/mL in synthetic serum and then the same methodology was applied. Again, data analysis with ImageJ allowed evaluation of the variation in each coordinate of the RGB system, and similar to the OPN buffer results, the red coordinate gave the best correlation, decreasing with increasing OPN concentration (Fig. 6).

In these tests, the linear range of response was between 5 and 1000 ng/mL, with a regression coefficient of 0.994. Despite the lower slope compared to the results observed in buffer, the calibration curve in undiluted serum provided a good response of color change as a function of OPN concentration, with a detectable difference between the control and the first standard concentration of 5 ng/mL. Furthermore, the same detection limit (LoD) and similar correlation coefficient values were obtained.

Other strategies for detecting OPN have been reported (Table S1). Lerner et al. [37], Sharma et al. [38], Meirinho et al. [29,39] and Zhou et al. [40] developed electrochemical biosensors that effectively detect OPN with LoD that can extend to the fM range, although clinical range for this biomarker goes between 20 ng/mL and 550 ng/mL [29]. Of these studies, only the ones developed by Meirinho et al. and Zhou et al. employed aptamers as biorecognition elements, which represent higher stability compared to antibodies. It is, however, important to note that the use of nanomaterials increases production costs and usually presents challenges when applied in a complex matrix, such as blood. Closer to the PoC requirements, is the study of Mukama et al. [28] that applies lateral flow principles to OPN detection. Since cellulose paper remains an attractive support material for its environmental and cost-effective features, this represented an interesting approach. Moreover, an aptamer was used as capturing element, which further reduces production cost and increases stability. However, as is common in lateral flow assays, gold nanoparticles functionalized with antibodies were still necessary as recognition elements, thus having the same limitations in terms of stability.

Compared to the presented strategies, this work represents a simpler approach and, as no antibodies or nanomaterials are used in its setup, the production costs and stability become more attractive. Moreover, the colorimetric response with quantification through smartphone camera makes this approach portable and user friendly. These are two fundamental features when it comes to a diagnosis device to be applied in any part of the world. Comparing to other quantification methods, like ELISA kits, this approach represents a faster and much less laborious method, since it only needs one sample incubation and one washing step, unlike ELISA where multiple washing steps, as well as incubation antibodies are required. Moreover, since it does not employ antibodies, it is much cheaper and can be performed at a fraction of the price. As far as this sensor's applicability in clinical practice, since the mentioned clinical range for this biomarker, the LoD and the linear interval achieved with this approach could be applied in a clinical context for cancer screening. For that, studies conducted with real samples would be necessary, in order to validate this assembly for diagnosis.

3.4.4. Spiked serum samples analysis

The recovery study with the aptasensor-based test strips was performed with serum samples spiked with known amounts of OPN (50.0 and 500.0 ng/mL). These specific concentrations were

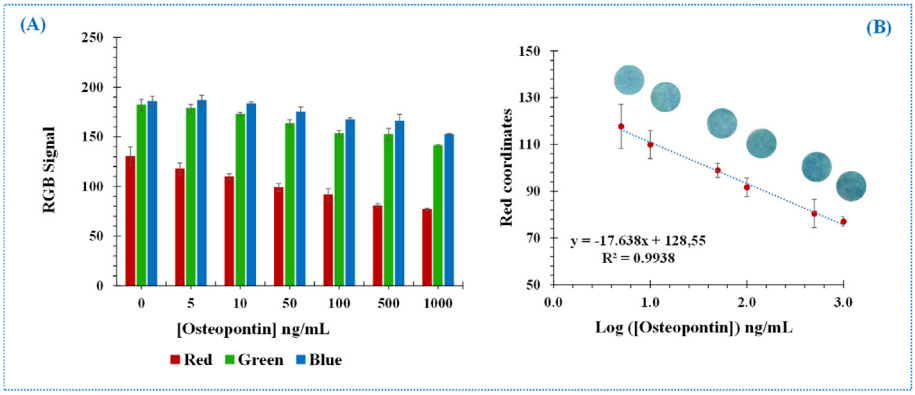

Fig. 6. Calibration curve for Osteopontin (OPN) in Cormay® synthetic serum. A: variation of the RGB (Red, Green, Blue) coordinates with the variation of OPN concentration; B: Calibration curve and linear equation for the red coordinates as a logarithm function of OPN's concentration from 5 to 1000 ng/mL. (For interpretation of the references to color in this figure legend, the reader is referred to the Web version of this article.)

Table 1
Results obtained from the recovery assay.

Prepared concentration (ng/ml)	Calculated concentration (ng/ml)	Recovered %
50	56	88
500	490	84

selected according to the studies of Bramwell et al. [41], which shows that the correlation between OPN levels in patients with recurrent or metastatic cancer has higher plasma OPN levels of 60.7 ng/mL, in a concentration range that may go up (23.9–543) in recurrences. The color was then recorded and the red coordinate was determined. The real concentration values calculated using the standard calibration curve were 56.0 and 490.0 ng/mL, respectively (Table 1). These values correspond to recoveries of 88.0 and 84.0%, respectively. Overall, this confirms the suitability of this test strip for the analysis of OPN in serum samples without the need for pre-dilution or sample pre-treatment.

4. Conclusions

In this work, a simple approach for colorimetric detection of OPN is presented. The design of the biosensor can be described as a two-step chemical modification: Silanization and aptamer binding. Since the final assembly already contains the revealing dye, only one incubation step with the target and one washing step are required for the application. Chemical modification of the cellulose with thiol groups allowed good covalent binding with the recognition element, and optimization of the detected signal allowed detection of OPN in both buffer and synthetic serum within clinical values. Overall, this aptasensor has the necessary sensitivity to be used for cancer screening. In addition, it is a highly attractive design with low-cost and stable materials in a portable structure that can be easily scaled up and used in many research areas.

Declaration of competing interest

The authors declare that they have no known competing financial interests or personal relationships that could have appeared to influence the work reported in this paper.

Acknowledge

This study was supported by the Portuguese Foundation for Science and Technology (FCT) under the scope of the strategic funding of UID/BIO/04469/2020 unit and BioTecNorte operation (NORTE-01-0145-FEDER-000004) funded by the European Regional Development Fund under the scope of Norte2020 - Programa Operacional Regional do Norte. Ana Cláudia Pereira is a recipient of a fellowship supported by a doctoral advanced training (call NORTE-69-2015-15) funded by the European Social Fund under the scope of Norte2020 - Programa Operacional Regional do Norte.

Appendix A. Supplementary data

Supplementary data to this article can be found online at https://doi.org/10.1016/j.aca.2022.339557.

References

[1] J. Li, J. Macdonald, Multiplex lateral flow detection and binary encoding enables a molecular colorimetric 7-segment display, Lab Chip 16 (2) (2016) 242–245.
[2] L. Anfossi, F. Di Nardo, S. Cavalera, C. Giovannoli, C. Baggiani, Multiplex lateral flow immunoassay: an overview of strategies towards high-throughput point-of-need testing, Biosensors (Basel) 9 (1) (2018).
[3] M.H. Ali, M.E. Elsherbiny, M. Emara, Updates on aptamer research, Int. J. Mol. Sci. 20 (10) (2019).
[4] F. Odeh, H. Nsairat, W. Alshaer, M.A. Ismail, E. Esawi, B. Qaqish, A.A. Bawab, S.I. Ismail, Aptamers chemistry: chemical modifications and conjugation strategies, Molecules 25 (1) (2019).
[5] S. Banik, S.K. Melanthota, Arbaaz, J.M. Vaz, V.M. Kadambalithaya, I. Hussain, S. Dutta, N. Mazumder, Recent trends in smartphone-based detection for biomedical applications: a review, Anal. Bioanal. Chem. 413 (9) (2021) 2389–2406.
[6] S. Arumugam, D.A.M. Colburn, S.K. Sia, Biosensors for personal mobile health: a system Architecture perspective, Adv Mater Technol 5 (3) (2020).
[7] D. Quesada-González, A. Merkoçi, Mobile phone-based biosensing: an emerging "diagnostic and communication" technology, Biosens. Bioelectron. 92 (2017) 549–562.
[8] Z. Geng, X. Zhang, Z. Fan, X. Lv, Y. Su, H. Chen, Recent progress in optical biosensors based on smartphone platforms, Sensors (Basel) 17 (11) (2017).
[9] Y. Gan, T. Liang, Q. Hu, L. Zhong, X. Wang, H. Wan, P. Wang, In-situ detection of cadmium with aptamer functionalized gold nanoparticles based on smartphone-based colorimetric system, Talanta 208 (2020) 120231.
[10] Y. Yao, C. Jiang, J. Ping, Flexible freestanding graphene paper-based potentiometric enzymatic aptasensor for ultrasensitive wireless detection of kanamycin, Biosens. Bioelectron. 123 (2019) 178–184.
[11] C.Y. Hui, M. Liu, Y. Li, J.D. Brennan, A paper sensor printed with multifunctional bio/nano materials, Angew Chem. Int. Ed. Engl. 57 (17) (2018) 4549–4553.
[12] W. Ji, Z. Zhang, Y. Tian, Z. Yang, Z. Cao, L. Zhang, Y. Qi, J. Chang, S. Zhang, H. Wang, Shape coding microhydrogel for a real-time mycotoxin detection system based on smartphones, ACS Appl. Mater. Interfaces 11 (8) (2019) 8584–8590.
[13] Z. Qiu, J. Shu, D. Tang, Bioresponsive release system for visual fluorescence detection of carcinoembryonic antigen from mesoporous silica nanocontainers mediated optical color on quantum dot-enzyme-impregnated paper, Anal. Chem. 89 (9) (2017) 5152–5160.
[14] R. Tian, J. Ji, Y. Zhou, Y. Du, X. Bian, F. Zhu, G. Liu, S. Deng, Y. Wan, J. Yan, Terminal-conjugated non-aggregated constraints of gold nanoparticles on lateral flow strips for mobile phone readouts of enrofloxacin, Biosens. Bioelectron. 160 (2020) 112218.
[15] C. Celik, G. Can Sezgin, U.G. Kocabas, S. Gursoy, N. Ildiz, W. Tan, I. Ocsoy, Novel anthocyanin-based colorimetric assay for the rapid, sensitive, and quantitative detection of, Anal. Chem. 93 (15) (2021) 6246–6253.
[16] S. Mittal, H. Kaur, N. Gautam, A.K. Mantha, Biosensors for breast cancer diagnosis: a review of bioreceptors, biotransducers and signal amplification strategies, Biosens. Bioelectron. 88 (2017) 217–231.
[17] A. Pereira, M. Sales, L. Rodrigues, Biosensors for rapid detection of breast cancer biomarkers, in: Inamuddin, A. Mohammad, R. Khan, A.M. Asiri (Eds.), Advanced Biosensors for Health Care Applications, Elsevier, 2019, pp. 71–103.
[18] B. Wei, K. Mao, N. Liu, M. Zhang, Z. Yang, Graphene nanocomposites modified electrochemical aptamer sensor for rapid and highly sensitive detection of prostate specific antigen, Biosens. Bioelectron. 121 (2018) 41–46.
[19] R. Tian, Y. Li, J. Bai, Hierarchical assembled nanomaterial paper based analytical devices for simultaneously electrochemical detection of microRNAs, Anal. Chim. Acta 1058 (2019) 89–96.
[20] Y.K. Yen, C.H. Chao, Y.S. Yeh, A graphene-PEDOT:PSS modified paper-based aptasensor for electrochemical impedance spectroscopy detection of tumor marker, Sensors (Basel) 20 (5) (2020).
[21] H. Wang, C. Zhou, X. Sun, Y. Jian, Q. Kong, K. Cui, S. Ge, J. Yu, Polyhedral-AuPd nanoparticles-based dual-mode cytosensor with turn on enable signal for highly sensitive cell evalution on lab-on-paper device, Biosens. Bioelectron. 117 (2018) 651–658.
[22] Y. Wang, J. Luo, J. Liu, S. Sun, Y. Xiong, Y. Ma, S. Yan, Y. Yang, H. Yin, X. Cai, Label-free microfluidic paper-based electrochemical aptasensor for ultrasensitive and simultaneous multiplexed detection of cancer biomarkers, Biosens. Bioelectron. 136 (2019) 84–90.
[23] M. Su, L. Ge, S. Ge, N. Li, J. Yu, M. Yan, J. Huang, Paper-based electrochemical cyto-device for sensitive detection of cancer cells and in situ anticancer drug screening, Anal. Chim. Acta 847 (2014) 1–9.
[24] L. Wu, C. Ma, L. Ge, Q. Kong, M. Yan, S. Ge, J. Yu, Paper-based electrochemiluminescence origami cyto-device for multiple cancer cells detection using porous AuPd alloy as catalytically promoted nanolabels, Biosens. Bioelectron. 63 (2015) 450–457.
[25] S. Ge, J. Zhao, S. Wang, F. Lan, M. Yan, J. Yu, Ultrasensitive electrochemiluminescence assay of tumor cells and evaluation of H, Biosens. Bioelectron. 102 (2018) 411–417.

[26] Y. Sun, S. Ge, J. Xue, X. Zhou, W. Lu, G. Li, X. Cao, Highly sensitive detection of cytochrome c in the NSCLC serum using a hydrophobic paper based-gold nanourchin substrate, Biomed. Opt Express 11 (12) (2020) 7062–7078.
[27] X. Cai, H. Zhang, X. Yu, W. Wang, A microfluidic paper-based laser-induced fluorescence sensor based on duplex-specific nuclease amplification for selective and sensitive detection of miRNAs in cancer cells, Talanta 216 (2020) 120996.
[28] O. Mukama, W. Wu, J. Wu, X. Lu, Y. Liu, J. Liu, L. Zeng, A highly sensitive and specific lateral flow aptasensor for the detection of human osteopontin, Talanta 210 (2020) 120624.
[29] S.G. Meirinho, L.G. Dias, A.M. Peres, L.R. Rodrigues, Electrochemical aptasensor for human osteopontin detection using a DNA aptamer selected by SELEX, Anal. Chim. Acta 987 (2017) 25–37.
[30] Y.Y. Xu, Y.Y. Zhang, W.F. Lu, Y.J. Mi, Y.Q. Chen, Prognostic value of osteopontin expression in breast cancer: a meta-analysis, Mol. Clin. Oncol. 3 (2) (2015) 357–362.
[31] P.H. Anborgh, L.B. Caria, A.F. Chambers, A.B. Tuck, L.W. Stitt, M. Brackstone, Role of plasma osteopontin as a biomarker in locally advanced breast cancer, Am. J. Transl. Res. 7 (4) (2015) 723–732.
[32] L.R. Rodrigues, J.A. Teixeira, F.L. Schmitt, M. Paulsson, H. Lindmark-Mänsson, The role of osteopontin in tumor progression and metastasis in breast cancer, Cancer Epidemiol. Biomarkers Prev. 16 (6) (2007) 1087–1097.
[33] P.H. Anborgh, D.J. Lee, P.F. Stam, A.B. Tuck, A.F. Chambers, Role of osteopontin as a predictive biomarker for anti-EGFR therapy in triple-negative breast cancer, Expert Opin. Ther. Targets 22 (8) (2018) 727–734.
[34] D. Loof, M. Hiller, H. Oschkinat, K. Koschek, Quantitative and qualitative analysis of surface modified cellulose utilizing TGA-MS, Materials (Basel) 9 (6) (2016).
[35] M. Abdelmouleh, S. Boufi, A. ben Salah, M.N. Belgacem, A. Gandini, Interaction of silane coupling agents with cellulose, Amer. Chem. Soc. (2002) 3203–3208.
[36] H. Koga, T. Kitaoka, A. Isogai, Chemically-modified cellulose paper as a microstructured catalytic reactor, Molecules 20 (1) (2015) 1495–1508.
[37] M.B. Lerner, J. D'Souza, T. Pazina, J. Dailey, B.R. Goldsmith, M.K. Robinson, A.T. Johnson, Hybrids of a genetically engineered antibody and a carbon nanotube transistor for detection of prostate cancer biomarkers, ACS Nano 6 (6) (2012) 5143–5149.
[38] A. Sharma, S. Hong, R. Singh, J. Jang, Single-walled carbon nanotube based transparent immunosensor for detection of a prostate cancer biomarker osteopontin, Anal. Chim. Acta 869 (2015) 68–73.
[39] S.G. Meirinho, L.G. Dias, A.M. Peres, L.R. Rodrigues, Development of an electrochemical RNA-aptasensor to detect human osteopontin, Biosens. Bioelectron. 71 (2015) 332–341.
[40] S. Zhou, M. Hu, X. Huang, N. Zhou, Z. Zhang, M. Wang, Y. Liu, L. He, Electrospun zirconium oxide embedded in graphene-like nanofiber for aptamer-based impedimetric bioassay toward osteopontin determination, Mikrochim. Acta 187 (4) (2020) 219.
[41] V.H. Bramwell, A.B. Tuck, J.A. Chapman, P.H. Anborgh, C.O. Postenka, W. Al-Katib, L.E. Shepherd, L. Han, C.F. Wilson, K.I. Pritchard, M.N. Pollak, A.F. Chambers, Assessment of osteopontin in early breast cancer: correlative study in a randomised clinical trial, Breast Cancer Res. 16 (1) (2014) R8.